Dynamic and structural insights into hydrogen-bonded interpolymer complexes of poly(2-alkyl-2-oxazolines) with poly(carboxylic acids)

Journal of Colloid and Interface Science 699 (2025) 138185

Contents lists available at ScienceDirect

Journal of Colloid And Interface Science

journal homepage: www.elsevier.com/locate/jcis

Regular Article

Dynamic and structural insights into hydrogen-bonded interpolymer complexes of poly(2-alkyl-2-oxazolines) with poly(carboxylic acids)

Ruslan Y. Smyslov [a], Yulia E. Gorshkova [b,c], Tatiana N. Nekrasova [a], Danelya N. Makhayeva [d], Grigoriy A. Mun [d], Galiya S. Irmukhametova [d], Vitaliy V. Khutoryanskiy [e,*]

[a] Institute of Macromolecular Compounds—Branch of B.P. Konstantinov Petersburg Institute of Nuclear Physics—NRC "Kurchatov Institute", Saint-Petersburg, Russia
[b] Joint Institute for Nuclear Research, Dubna, Russia
[c] Institute of Physics, Kazan Federal University, Kazan, Russia
[d] Faculty of Chemistry and Chemical Technology, al-Farabi Kazakh National University, Almaty 050040, Kazakhstan
[e] Reading School of Pharmacy, University of Reading, Whiteknights, PO Box 224, Reading, United Kingdom

HIGHLIGHTS

- Interpolymer complexes between PAOx and PMAA were studied in aqueous and methanol solutions.
- The length of the alkyl side chain in PAOx influences its binding affinity with PMAA.
- Relaxation times quantifying local mobility of PMAA increased from 80 to 680 ns upon complexation.
- SAXS analysis reveals a single hierarchical level of IPC supramolecular structures ranging from 4 to 10.7 nm.
- The compactness of the supramolecular structure is governed by a hydrogen-bonding network.

GRAPHICAL ABSTRACT

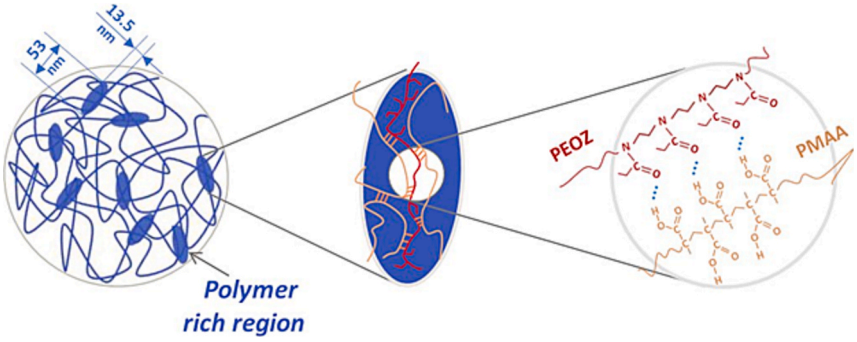

ARTICLE INFO

Keywords:
Nanosecond dynamics
H-bonds
Water soluble polymers
Interpolymer complexes
Polarized luminescence
SAXS

ABSTRACT

The formation of interpolymer complexes (IPCs) between poly(2-alkyl-2-oxazolines) (PAOx) and poly(methacrylic acid) (PMAA) in solutions has been investigated using polarized luminescence relaxation and small-angle X-ray scattering (SAXS) structural methods. The results reveal that hydrophobic interactions contribute to the formation of IPCs in both aqueous and methanol solutions, influenced by the length of the side group in PAOx. The relaxation times, which can be used to quantify the intramolecular mobility of the luminescently labeled poly(methacrylic acid) (PMAA*), increase from 80 to 680 ns, indicating the formation of IPCs between PMAA* and PAOx. SAXS analysis of aqueous IPC solutions unveils their supramolecular organization, which is similar to that of nanohydrogels, with the hierarchical level comprising compact structures ranging from 4 to 10.7 nm in size.

* Corresponding author at: Reading School of Pharmacy, University of Reading, Whiteknights, PO Box 224, RG6 6AD Reading, United Kingdom.
E-mail address: v.khutoryanskiy@reading.ac.uk (V.V. Khutoryanskiy).

https://doi.org/10.1016/j.jcis.2025.138185
Received 15 May 2025; Received in revised form 8 June 2025; Accepted 11 June 2025
Available online 13 June 2025

1. Introduction

Interpolymer complexes (IPCs) constitute a distinct class of polymeric materials, exhibiting properties that differ markedly from those of their constituent polymers [1–4]. These materials are increasingly used in drug delivery systems, encapsulation technologies, surface modification, water purification, sensor and membrane technologies [5–11]. The four main classes of interpolymer complexes include those stabilized by electrostatic interactions (polyelectrolyte complexes) [12,13], hydrogen bonding (H-bonded IPCs) [14–16], stereocomplexation between stereoisomers (stereocomplexes) [1,17–20], and charge-transfer interactions (charge-transfer complexes) [21]. These complexes can be prepared by mixing individual polymers in aqueous or organic solutions, polymerizing monomers in the presence of complementary macromolecules (template polymerization), or through self-assembly at interfaces, such as via the layer-by-layer deposition technique [22,23] or at liquid–liquid boundary [24].

The formation of interpolymer complexes in solutions is a multifaceted and multistage self-assembly process driven by primary interactions, complemented by secondary forces such as hydrophobic (solvophobic) effects, solvation and desolvation of individual macromolecules. These factors contribute to macromolecular contraction, leading to the formation of compact structures with reduced mobility. Studies on complex formation in these systems can also provide valuable insights into self-assembly phenomena in biological systems, such as proteins, nucleic acids, and polysaccharides [25].

Despite several decades of research on interpolymer complexes, many aspects of their formation and structural organization remain poorly understood. This is particularly true for hydrogen-bonded interpolymer complexes formed between poly(carboxylic acids) and proton-accepting non-ionic polymers. One of the earliest studies on hydrogen-bonded IPCs was conducted by Smith et al. in 1959 [26], who reported association reactions between poly(carboxylic acid)s and poly (alkylene oxide). Since then, hundreds of publications have detailed the formation of complexes between poly(carboxylic acids) and various non-ionic polymers, including polyethylene oxide [27–29], poly(vinyl alcohol) [30], polyacrylamide and its derivatives [31–33], poly(*N*-vinylpyrrolidone) [34–37], cellulose ethers [38], and other polymer classes [39].

Historically, the formation of hydrogen-bonded complexes in solutions was studied using various physicochemical methods, including measurements of viscosity, conductivity, pH, solubility, and turbidity. The structure of these complexes was investigated using microscopic techniques such as scanning electron microscopy (SEM) and transmission electron microscopy (TEM). Later advancements in physicochemical techniques provided additional tools for structural, thermodynamic, and kinetic studies of IPCs, including dynamic light scattering, isothermal titration calorimetry, surface plasmon resonance, and fluorescent methods including polarized luminescence [1,40–43].

Poly(2-alkyl-2-oxazolines) (PAOx) are an emerging class of polymers that have gained significant attention from researchers over the past few decades [44–46]. The interest in these polymers arises from their controlled synthesis via ring-opening polymerization, as well as the ability to tailor their macromolecular architecture and hydrophobic-hydrophilic balance. Several representatives of PAOx are fully soluble in water, and their non-toxic nature offers promising opportunities for biomedical applications [47–49]. Examples of these applications include polymer-drug conjugates [50], micellar drug carriers [51–53], thermoresponsive systems [54], solid drug dispersions [55,56], mucoadhesive polymers and formulations [7,57], hydrogels [58,59], and antimicrobial iodophors [60].

Water-soluble poly(2-alkyl-2-oxazolines) have strong proton-accepting properties, making them capable of forming hydrogen-bonded interpolymer complexes with poly(carboxylic acids). However, compared to many other water-soluble polymers, the complexes formed by PAOx have received relatively little attention until recently, with most studies focusing primarily on their applications. For example, Moustafine et al. [61] and Ruiz-Rubio et al. [62] investigated the formation of complexes between poly(2-ethyl-2-oxazoline) and weakly cross-linked poly(acrylic acid) (Carbopol® 971), using them to formulate solid dosage forms for oral and buccal drug delivery, respectively. Adatoz et al. [63] reported the use of interpolymer complexation between poly(2-ethyl-2-oxazoline) and tannic acid to form multilayered fibers and films. Su et al. [64] used layer-by-layer self-assembly between poly(2-ethyl-2-oxazoline) and poly(acrylic acid) to form thin films. Moon et al. [65] reported the preparation of supramolecular adhesive gels based on interpolymer complexation between poly(2-ethyl-2-oxazoline) and tannic acid.

In the present study, we explore the formation and structural features of interpolymer complexes formed by poly(methacrylic acid) (PMAA) and poly(2-methyl-2-oxazoline) (PMOx), poly(2-ethyl-2-oxazoline) (PEOx), and poly(*n*-propyl-2-oxazoline) (PnPOx). The use of these three derivatives offers a unique opportunity to assess the impact of the hydrophobic-hydrophilic balance of non-ionic polymers on the structure of the IPCs and the intramolecular mobility (IMM) of macromolecules within their self-assembled structures. Two advanced methods of physicochemical characterization such as polarized luminescence and small angle X-ray scattering were used to evaluate these structural features and molecular mobility within interpolymer complexes [66–68].

2. Experimental Section

2.1. Materials

PEOx with a molecular weight of 50 kDa ($Đ = 3–4$), purchased from Sigma-Aldrich, was used without any purification (CAS No. 25805–17-8, Product No. 372,846 and 373974). The following reagents were also used without prior purification: triethylamine (TEA) (Sigma-Aldrich), acetic anhydride (Across Organics), butyric anhydride (Merck), and N, *N*-dimethylacetamide (DMA) (Reagent Plus). These reagents were selected based on their purity levels, with a minimum purity of 99 %.

2.2. Synthesis of poly(2-methyl-2-oxazoline) and poly(n-propyl-2-oxazoline)

In this study, PMOx and PnPOx were synthesized via acid hydrolysis of PEOx followed by acylation, with slight modifications to a previously reported method [5,69]. Commercial-grade PEOx (50 kDa, DP ~ 505) was hydrolyzed in 18 % HCl at 100 °C for 14 h to prepare linear polyethyleneimine (PEI). The solution was then neutralized with NaOH (pH 10–11), and the precipitate was filtered, washed, and vacuum-dried. The dried PEI (1 g) was dissolved in DMA (20 mL), heated to 50 °C for complete dissolution of PEI, and then cooled to a room temperature. Acetic or butyric anhydride (1–1.5 equiv.) with TEA (1–1.5 equiv.) was added dropwise under nitrogen and stirred for 14 h. The product was purified via dialysis against deionized water (MWCO 12–14 kDa) and then freeze-dried.

The commercial PEOx and the synthesized PMOx were analyzed using gel-permeation chromatography using Viscotek (Malvern Instruments, UK) chromatograph equipped with 270 dual detector (Malvern) and VE 3580 RI detector (Malvern Instruments, UK). However, due to poor solubility of PnPOx in 0.1 M $NaNO_2$ solution and its thermosensitivity above 24 °C, this polymer could not be analyzed. PEOx had a molecular weight of 64.4 kDa, differing from the manufacturer's reported 50 kDa, while PMOx had a molecular weight of 36.8 kDa, aligning with expected chemical transformations. FTIR spectra of dry PEOx, PMOx, PnPOx and PEI were recorded on Nicolet iS5 FTIR spectrophotometer with a DTGS detector and 1H NMR spectra were recorded in solutions using DPX 400 MHz NMR spectrophotometer Bruker (Germany). FTIR and 1H NMR spectra of PEI, PMOx and PnPOx and results of GPC are provided as Figs. S2–S4 and Table S1 in the Supporting information.

2.3. Synthesis of luminescently labeled poly(methacrylic acid)

In this study, two forms of PMAA were used: one that was not labeled and one that was luminescently labeled (PMAA*). The latter was used in experiments with the polarized luminescence. The preparation of PMAA* involved the free-radical copolymerization of methacrylic acid (MAA) and 9-anthryl methylmethacrylamide (9-AMA) (Scheme S2 in Supporting information), as previously reported [42]. The free-radical copolymerization reaction was carried out in sealed ampoule in an argon atmosphere at 60 °C with 1 g MAA (11.5 mmol) and 10 mg of 9-AMA (36.3 μmol) dissolved in 5 mL N,*N*-dimethylformamide (Sigma-Aldrich, St. Louis, MO, USA) with 10 mg (60 μmol) of 2,2′-azobisisobutironitrile (AIBN, Sigma-Aldrich, St. Louis, MO, USA) as an initiator for 24 h. The 9-AMA were used as luminescent labels. Subsequently, the copolymer solution was purified from low molecular weight impurities by dialysis against deionized water. The purification process employed Spectra/Por 7 dialysis membranes (MWCO 1 kDa, Spectrum Laboratories, Inc., USA). The final product was subsequently lyophilized. The yield of PMAA* was 0.84 g (84 %).

The content of luminescent labels (LL) in PMAA* was determined by UV–Vis spectrophotometry with the use of an SF-256 UVI spectrophotometer ("LOMO Photonika Ltd.", Saint Petersburg, Russia) at 365 nm. The value of the molar extinction coefficient, ε, of 9-AMA at 368 nm was equal to 8300 $cm^2 \cdot mmol^{-1}$. The LL content was determined to be 0.15 mol%, thereby excluding the appearance of photophysical processes such as migration of electron excitation energy or formation of excimers, which would otherwise give erroneous values of luminescence polarization.

The molecular weight of PMAA* was calculated from the values of diffusion coefficients D and sedimentation coefficients s, measured in 0.1 N NaCl solution at 24 °C, according to the Svedberg equation:

$$M_{sD} = (s/D)RT/(1 - \bar{\nu}\rho_0) \quad (1)$$

where R is the universal gas constant, T is the absolute temperature, $\bar{\nu}$ is the partial specific volume determined by pycnometry, and ρ_0 is the medium density [70,71]. The molecular weight M_{sD} of the studied PMAA* samples was determined to be 267 kDa.

2.4. Characterization

The nanosecond relaxation times, τ_{IMM}, which are indicative of the intramolecular mobility of PMAA* macromolecules, were determined by measuring the luminescence polarization (P) of the solution according to the following equation [66]:

$$\tau_{IMM} = 3 \cdot \frac{1/P_0' + 1/3}{1/P - 1/P_0'} \cdot \tau_{fl}, \quad (2)$$

where τ_{fl} is the fluorescence lifetime of the luminescent label (anthracene-containing group) and $1/P_0'$ is a parameter taking into account the contribution of high-frequency movements of the luminescent label (Fig. S1 in Supporting information). The concentration of PMAA* in the solution was c_{pol} = 0.5 $g \cdot L^{-1}$. The concentration of PAOx solutions added with careful stirring was 8–10 $g \cdot L^{-1}$ to minimize dilution of the initial PMAA* solution.

SAXS experiments were performed at the Frank Laboratory of Neutron Physics (FLNP) of JINR (Dubna) on the Xeuss 3.0 laboratory facility (Xenocs, France). The Xeuss 3.0 universal X-ray scattering system is equipped with the GeniX^{3D} X-ray beam delivery system, which produces high intensity monochromatic Cu K_α X-rays. The scattered signal of the radiation passing through the sample is measured by a megapixel (1 M) position sensitive Dectris Eiger2 R detector. Three detector-sample positions were used in the experiment: 300, 2000 and 4200 mm, which allowed us to study the IPC in the ultrasmall angle X-ray scattering (USAXS) and SAXS modes over a range of momentum transferred, q, from 0.06 to 8 nm^{-1}. The SAXS data are presented as the dependence of the scattering intensity $I(q)$ on the momentum transferred q, defined by the relation:

$$q = 4\pi \sin\theta/\lambda, \quad (3)$$

where θ is the half of the scattering angle (2θ) and λ is the wavelength of the incident X-rays.

IPC solutions for SAXS measurements were prepared in distilled water at a polymer concentration of 8 $g \cdot L^{-1}$. The PAOx/PMAA component ratio was 1/1 as a unit-mol ratio. Three aqueous solutions were prepared with the following compositions: PMOx/PMAA, PEOx/PMAA, and PnPOx/PMAA sealed within 1.5 mm diameter borosilicate glass capillaries and measured at room temperature under vacuum. Data acquisition time ranged from 20 to 40 min, depending on the detector-sample distance.

3. Results and discussion

3.1. Polarized luminescence of IPC solutions

The polarized luminescence (PL) method is a photophysical approach [41,66,72,73] that provides an opportunity to study the formation and structure of IPC by measuring nanosecond relaxation times (τ_{IMM}), which are characterizing the intramolecular mobility of the macromolecules (Eq. 1). Intramolecular mobility has been found to be associated with relaxation processes involving macromolecular segments. It has been previously demonstrated that both intra- and intermolecular interactions are reflected in the changes in relaxation times, which variation is attributable to the nanosecond-range duration of the luminescence emission, τ_{fl} [1,41,66]. This approach is possible by evaluating the change in the inverse value of the luminescence polarization, $1/P$, of the solution containing the polymers with covalently attached luminescent labels representing an anthracene core (Equation 2 and Fig. S1 in Supporting information).

Fig. 1 shows the changes in nanosecond relaxation times, τ_{IMM}, of PMAA* macromolecules in water upon addition of poly(2-alkyl-2-oxazoline) solutions. The addition of PAOx to the polyacid solution results in a substantial increase in the values of τ_{IMM}, indicating a

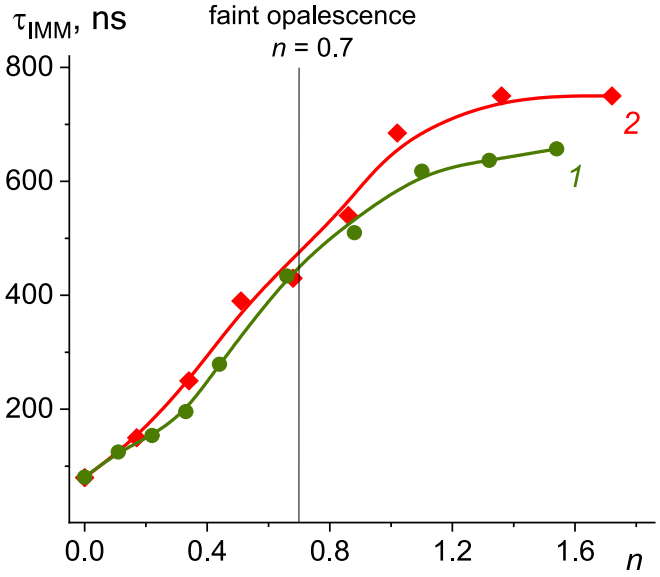

Fig. 1. Dependence of τ_{IMM} for PMAA* in complexes with PMOx (*1*), PEOx (*2*) on the ratio of n = $[PAOx]_{SRU}/[COOH]$ in aqueous solution. The value of τ_{IMM} are presented at T/η = 335 K•cP^{-1}. The plotting is facilitated by the Origin software product (version 2025, OriginLab Corporation, Northampton, MA, USA).

concomitant decrease in the mobility of polyacid chain segments. These changes indicate the occurrence of interactions with PAOx and the subsequent formation of IPC. The formation of IPC between PMAA* and PAOx is driven by H-bonding between the non-ionized proton-donating carboxyl groups (COOH) and the proton-accepting carbonyl oxygen present in PAOx.

The opalescence was observed in aqueous solutions when the ratio of interacting components, *n*, was around 0.7 indicating the aggregation of the formed IPCs. This is likely attributable to the formation of a cooperative system of hydrogen bonds between individual macromolecules upon interaction of the polyacid with PAOx (Scheme 1). In the absence of geometric correspondence, hydrogen bonds are formed between distant, disconnected groups in interacting polymer chains. At $n > 0.7$, numerous H-bonds (crosslinks) are formed between particles representing IPC. This interaction leads to the formation of a network structure for intermolecular aggregates. The formation of this structure appears to be attributable to steric factors, namely the distance between interacting groups and the presence of substantial hydrophobic substituents, which hinders the development of an extensive H-bond system.

A gradual addition of poly(2-oxazoline) solutions to PMAA initially results in a fast linear growth in τ_{IMM} values until the molar ratio of polymers, *n*, reaches 1 (Fig. 1, where curves *2* and *3* are juxtaposed). Then further addition of non-ionic polymers results in a less pronounced increase in τ_{IMM}. This is likely related to 1:1 stoichiometry of the IPCs formed, when each carboxylic group of PMAA forms an H-bond with a proton-accepting group of PAOx. This IPC stoichiometry is also in agreement with the previous reports, when similar systems were studied [72]. A comparison of τ_{IMM} values measured when the *n* is equal to 1 for the two IPCs formed by different poly(2-oxazolines) provides information about the role of hydrophobic effects in the complex formation. The observed dependence of τ_{IMM} values on the length of the alkyl side chain in PAOx provides evidence that the formation of a compact IPC structure is not solely governed by hydrogen bonding between proton-donor and acceptor groups. Instead, it also involves significant contributions from hydrophobic interactions between the PAOx alkyl chains and the PMAA* backbone. This is illustrated by the increase in τ_{IMM} from 580 ns for the IPC formed by PMOx with PMAA* to 680 ns for the IPC formed by PEOx with PMAA* (at $n = 1$). In non-ionized conditions, the α-methyl groups of PMAA contribute to the formation of hydrophobic domains in aqueous solution, which in turn impose considerable steric hindrance on polymer chain mobility—greater than that observed for poly(acrylic acid), for example. The interaction between these hydrophobic α-methyl domains and the alkyl radicals of PAOx leads to the development of a more compact IPC structure. This enhances steric constraints and correspondingly reduces the mobility of PMAA*. The effect becomes more pronounced with increasing hydrophobicity of the PAOx component. The role of hydrophobic interactions involving PMAA and poly (acrylic acid) has been previously demonstrated in [72].

It is well known that the formation of hydrogen-bonded IPC between poly(carboxylic acids) and non-ionic proton-accepting polymers usually occurred when the carboxylic groups of proton-donating polymer (polyacid) are unionized. Therefore, the measurement of inversed polarized luminescence values ($1/P$) as a function the degree of ionization of PMAA may provide an information about the stability of IPCs. In the following experiments the dependence of $1/P$ value for PMAA* alone

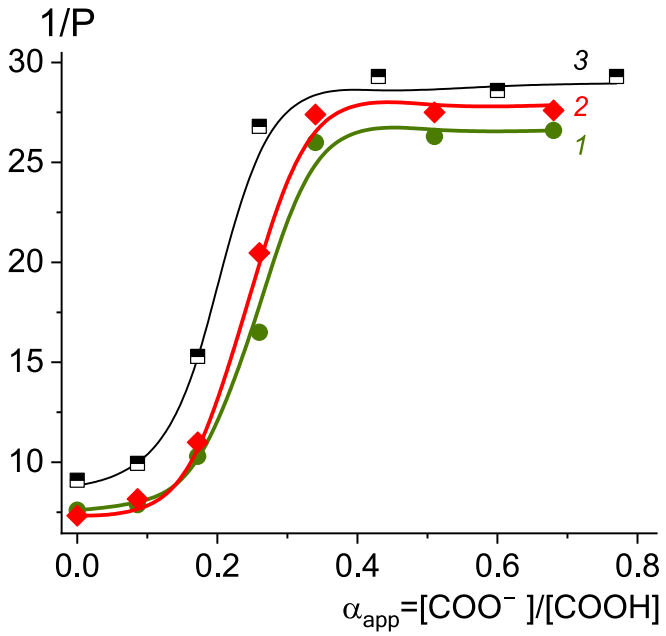

Fig. 2. Dependence of $1/P$ value for PMAA* in complexes with PMOx (*1*), PEOx (*2*), and individual PMAA* (*3*) in aqueous solutions on the apparent degree of ionization, α_{app}, at $n = [PAOx]_{SRU}/[COOH] = 1.5$.

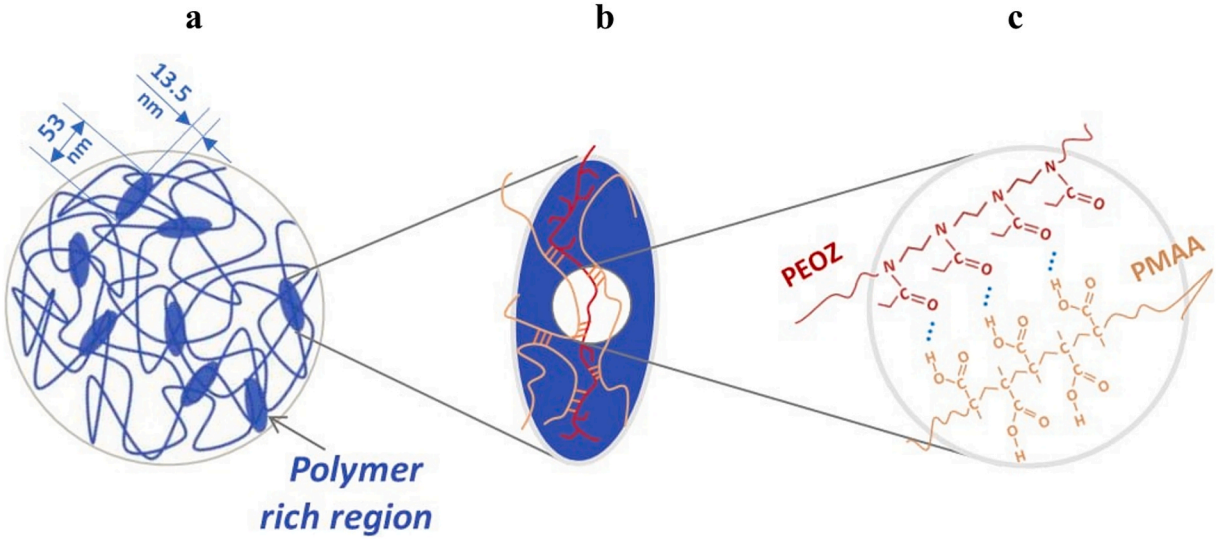

Scheme 1. Proposed supramolecular structure of the complex between PMAA and PEOx on the mesoscopic level (a), for a two-stranded structure (b), and the structure of H-bonds (c).

and within the IPC formed with PEOx and PMOx was determined as a function of the degree of ionization of carboxylic groups (Fig. 2). It is important to note that PMAA is a weak polyelectrolyte, and in aqueous solution without adjustment of pH values, the apparent degree of ionization, α_{app}, of COOH groups does not exceed 0.03 [72]. In the non-ionized and weakly ionized state, the PMAA macromolecules take more compact conformation that is stabilized by hydrogen bonds and hydrophobic interactions of α-methyl groups [72]. This is confirmed by relatively large values of relaxation times, indicating the reduced intramolecular mobility of PMAA macromolecules. These relaxation times have been determined to be approximately 80 ns. As a result, the intramolecular mobility of PMAA chains is significantly hindered compared to, for example, poly(acrylic acid) [72]. PMAA ionization has been shown to increase the mobility of polymeric chain segments as seen from the decrease in τ_{IMM}. This phenomenon can be attributed to the destruction of the compact structure due to electrostatic repulsion between negatively charged carboxylate ions. The τ_{IMM} of around 10 ns is observed for fully ionized PMAA*. Fig. 2 shows that a sharp increase in $1/P$ values in the IPCs is observed at larger degree of ionization of COOH groups. Furthermore, it should be noted that at elevated degrees of ionization, PMAA* macromolecules are not fully released from IPC with PAOx. The longer the alkyl radical in poly(2-alkyl-2-oxazoline), the more pronounced the disparity between the $1/P$ value for PMAA* and PAOx (cf. curves *1*, *2*, and *3* in Fig. 2). It indicates that compact structure of IPC and restrained mobility of PMAA* macromolecules are retained at larger degrees of ionization. However, a comparison of the complexes formed by PAOx and PMAA in this study with the literature data on the IPC formed by poly(*N*-vinylpyrrolidone) and PMAA reveals that poly(2-oxazolines) form noticeably less stable complexes, which exist in a narrower range of pHs [41].

The IPC formed by PEOx shows a slightly higher stability compared to the complex formed by PMOx, which is likely to be related to additional contribution of hydrophobic effects, whose role is more pronounced for poly(2-ethyl-2-oxazoline) (cf. curves *2* and *3*, Fig. 2).

It is well-known that formation of hydrogen-bonded IPC is also possible in some organic solvents. The use of organic solvents such as methanol provides an opportunity to study a wider range of poly(2-oxazolines), for example, including poly(*n*-propyl-2-oxazoline), whose solubility in water was limited. Subsequent experiments were conducted to study formation of complexes of PMAA* with PMOx, PEOx and PnPOx in methanol. Figs. 3 and 4 illustrate the changes in the $1/P$ values of the PMAA* solution and the τ_{IMM} values for PMAA* macromolecules upon addition of different poly(2-alkyl-2-oxazolines) in methanol. A pronounced opalescence was observed in the solution mixtures of PMOx and PEOx with PMAA* when the ratio of the interacting components was $n \geq 0.3$–0.4. The aggregation of IPC prevents further measurements of luminescence polarization at higher PAOx/PMAA* ratios.

As illustrated in Figs. 3 and 4, the addition of PAOx solution to PMAA* in methanol results in a decrease in $1/P$ values and an increase in τ_{IMM} for PMAA* macromolecules, respectively. This observation indicates the occurrence of an interaction between PMAA* and PAOx macromolecules, leading to the formation of interpolymer complex between these polymers. In contrast to aqueous solutions, where the formation of IPC is weakly dependent on the structure of PAOx, a significant influence of the nature of the substituent on the interaction with PMAA* is observed in methanol (cf. Figs. 1 and 4). The values of $1/P$ and τ_{IMM} change weakly with increasing values of n when poly(*n*-propyl-2-oxazoline) is added to PMAA* solution, but when poly(2-ethyl-2-oxazoline) and poly(2-methyl-2-oxazoline) is added, the $1/P$ values of PMAA* solution drop sharply, and the value of τ_{IMM} increases (cf. Figs. 3 and 4). In addition, opalescence in methanol appears at much lower values of n than in water, equal to 0.3 and 0.4 for PMAA complexes with PMOx and PEOx, respectively. It can be hypothesized that in methanol, where all alkyl groups are exposed to the solvent, as the substituent size increases, steric hindrance arises for the interaction of the carbonyl oxygen of PAOx with the COOH groups of PMAA. From the comparison of τ_{IMM} values in water and methanol, it can be concluded that a 'looser' structure is formed in methanol. In addition, in contrast to water as a solvent, in which a more hydrophobic group enhances the PAOx/PMAA interaction, in methanol the observation is opposite and interactions between the polymers become weaker. These results correlate well with the data on the formation and stability of poly(acrylic acid) complexes with copolymers of vinyl butyl ether and vinyl ether of ethylene glycol (VBE-VEEG) in aqueous and organic solvents [74]. It has been shown in [74] that the copolymers containing more hydrophobic VBE units in the copolymer chain tended to form more stable complexes in aqueous solutions due to the contribution of hydrophobic interactions. At the same time, the opposite trend was observed in isopropanol: IPCs formed by

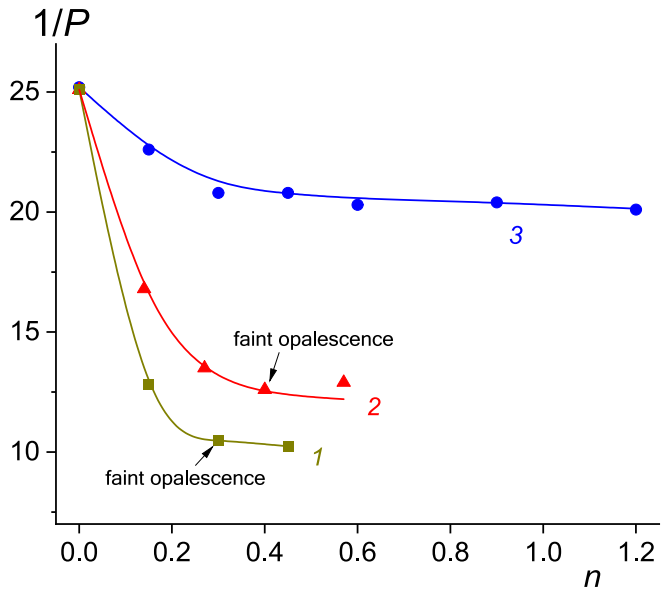

Fig. 3. Dependence of $1/P$ value of PMAA* upon the interaction with PAOx in methanol on the ratio of $n = [PAOx]_{SRU}/[COOH]$ in methanol for PMOx (*1*), PEOx (*2*), and PnPOx (*3*).

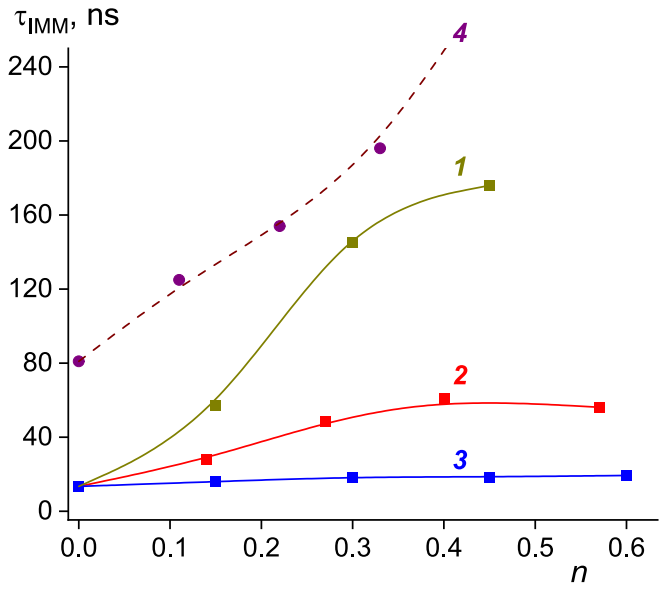

Fig. 4. Dependence of the PMAA* τ_{IMM} values in complexes with PMOx (*1*), PEOx (*2*), and PnPOx (*3*) on the ratio of $n = [PAOx]_{SRU}/[COOH]$ in methanol. For comparison, the values of τ_{IMM} for PMAA* macromolecules in aqueous solution are presented (*4*). All τ_{IMM} are reduced to water viscosity values at $T/\eta = 335$ K•cP^{-1}.

the copolymers with a greater content of VBE showed lower stability.

3.2. Small-angle X-ray scattering

Unlike polarized luminescence technique, SAXS method can be used for colloidal solutions with some aggregation. However, this method is less sensitive and requires the use of polymers at reasonably high concentrations. In this study, the aqueous solutions of IPC with the polymers' concentration of 8 mg·mL^{-1} were examined using SAXS method. To analyze the structure and shape of the formed macromolecular systems, three different approaches to process the scattering data were employed (Fig. 5). The dependence of the scattering intensity, $I(q)$, on the scattering vector, q, was plotted in a double logarithmic scale (5a). A Kratky plot was generated (5b), and a size distribution of scattering particles in "direct" space was calculated (5c). To analyze the SAXS curves (Fig. 5a), the model proposed by Beaucage for systems with a single-level structural organization was employed [75]:

$$I(q) = G\cdot\exp\left(-\frac{q^2R_{gG}^2}{3}\right) + B\left(\frac{\left(\mathrm{erf}\left(qR_{gG}/\sqrt{6}\right)\right)^3}{q}\right)^{\nu} + I_{bg} \quad (4)$$

where R_{gG} is the radius of gyration, ν is the Porod exponent corresponding to the fractal dimension of the scattering inhomogeneities, G is the Guinier prefactor, and B is the pre-exponential factor. Parameter I_{bg} is responsible for background scattering. The experimental derivation of intensity relationships $I(q)$ on the momentum transferred, q, was accomplished through the implementation of the least mean square method over the entire range of measured q values. This was performed using SasView software [76]. The quality of the fit of the experimental curves was evaluated by the parameter $\chi^2_{reduced}$ (reduced chi-squared) defined as

$$\chi^2_{reduced} = \sum\left((I(q)_{meas} - I(q)_{calc})^2/E(q)^2\right)/(N_{pts} - N_{params})$$

where $E(q)$ is the error of the intensity value $I(q)$, N_{pts} is the number of data points in the data set, N_{params} is the parameter number for the optimized model.

The interaction of PAOx with PMAA results in the formation of a supramolecular structure of the IPC in solution. As illustrated in the inset of Fig. 5a, the zero-extrapolated angle scattering intensity, $I(0)$, of aqueous solutions of PAOx/PMAA increases in accordance with an increase in the hydrophobicity of the side group (Scheme S1), with the side groups being methyl, ethyl and *n*-propyl (Fig. 5a). The observed phenomenon can be attributed to the presence of a α-methyl group within the structure of PMAA. This group facilitates the hydrophobic interactions within the interpolymer complex that exists between PMAA and PAOx. The consequence of these interactions is the compaction of the structure of PMAA. It was determined that as the hydrophobicity of the alkyl groups increases from methyl, ethyl to *n*-propyl (Scheme S1), the radius of gyration, R_{gG}, for the supramolecular IPC structure (Equation 3) increases from 12.1, 15.3 to 16.5 nm (Table 1).

In the context of the real space, the particle sample in question can be most conveniently described by the distance distribution function $P(r)$, where r is the scattering center spacing. This function can be presented as a histogram that quantifies the distance between all possible pairs of atoms within the specified particle. It is the inverse Fourier transformation for the small-angle scattering function $I(q)$ in the spherical system of coordinates [75,77–79]:

$$P(r) = \frac{r^2}{2\pi^2}\int_0^{\infty} q^2 I(q)\frac{\sin(qr)}{qr}dq. \quad (5)$$

Given the specified condition: $P(r) \equiv 0$, at $r \geq D_{max}$ (Fig. 5c), an estimate of D_{max} value can be obtained. This evaluation of D_{max} value was instrumental in determining the maximum size of IPC. The latter for these complexes was determined to be increased: 43, 51 and 65 nm for

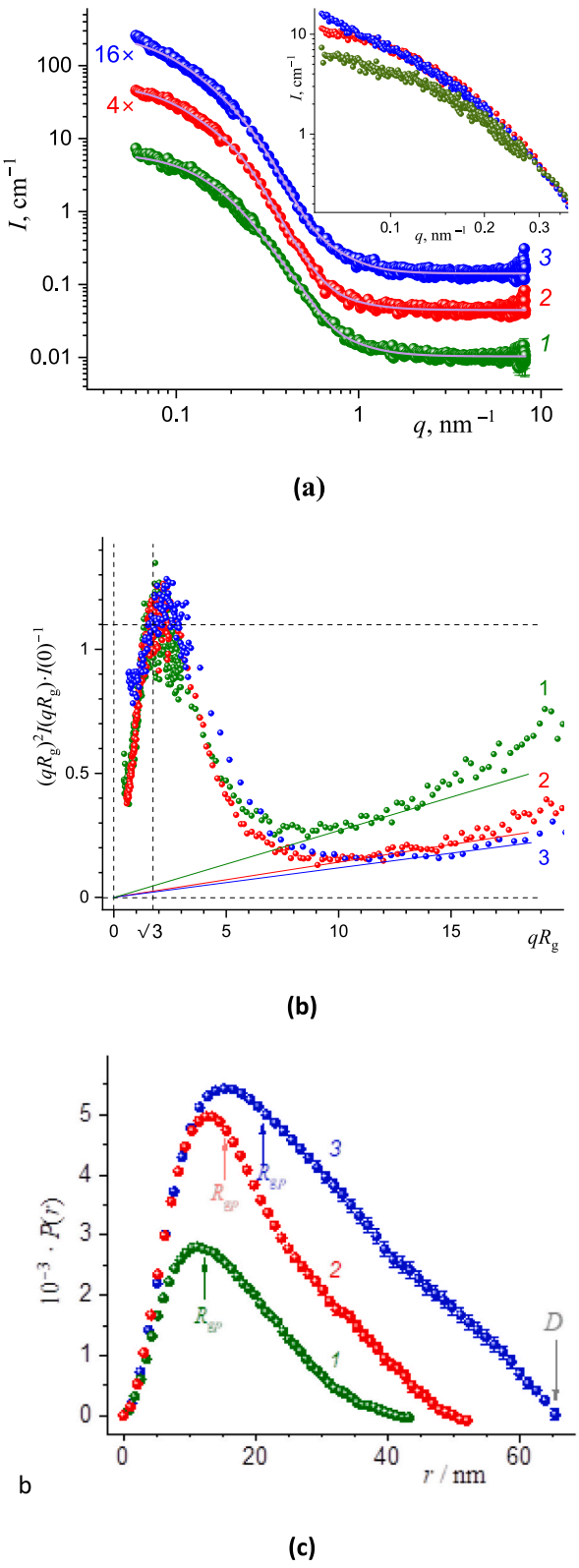

Fig. 5. SAXS curves presented in double logarithmic coordinates (a) and in Kratky plot (b); the distance distribution function (c) for PMOx/PMAA (*1*), PEOx/PMAA (*2*), and PnPOx/PMAA (*3*). The light purple curves in part (a) represent the result of the approximation by the Beaucage function (Eq. 4). The arrows indicate the radii of gyration, as determined by Eq. 5 (Table 1). (For interpretation of the references to colour in this figure legend, the reader is referred to the web version of this article.)

Table 1
The parameters of IPC formed between PMAA and PAOx as calculated from the results of SAXS measurements based on approximation by a one-level unified Beaucage function (Eq. 4) [75] and analyzing the distance distribution function, P(r), (Eq. 5) [77].

Parameters	PMOx/PMAA	PEOx/PMAA	PnPOx/PMAA
D_p (nm)	44 ± 1	53 ± 1	65 ± 1
D_{eq} (nm)	11.2	13.5	15.3
R_{gp} (nm)	12.4 ± 0.2	15.3 ± 0.2	21.2 ± 0.2
R_{gG} (nm)	11.1 ± 0.1	13.7 ± 0.6	16.0 ± 2.3
$\nu = 4 + 2\beta$ *or*	–	4.70 ± 0.03	4.31 ± 0.03
$6 - d_s$ [83]	3.986 ± 0.003	–	–
$\chi^2_{reduced}$	1.2	1.3	1.2

the complexes formed by PMOx, PEOx and PnPOx, respectively (Table 1). The radius of gyration relative to the center of mass of the system, R_{gp}, was obtained from the $P(r)$ by calculating the ratio of the second moment to the "zero" one, i.e., the mean square of the distances r between the scattering centers [75]:

$$R_{gp}^2 = \frac{1}{2}\int_0^{D_{max}} r^2 P(r)dr \Big/ \int_0^{D_{max}} P(r)dr. \quad (6)$$

The values of the radius of gyration, R_{gp}, calculated according to the previously stated expression, are presented in Table 1. The R_{gp} values, as well as the R_{gG} values calculated by the single-level unified Beaucage function (Eq. 4), increase with the length of the alkyl side groups of the PAOx. However, it should be noted that in all cases, $R_{gp} > R_{gG}$. This phenomenon is analogous to what is observed in flexible and unfolded systems, such as biopolymers [80]. Furthermore, the profile of distance distribution function, $P(r)$, of the scattering particles can be used to ascertain the shape of the scattering objects [75]. The globular compact particles have a symmetrical bell-shaped distribution $P(r)$, while less compact (unfolded) particles have an elongated tail [79,81]. In this case, it is reasonable to assume that the IPCs can be presented as a two-axis ellipsoid, where D_p is the polar diameter, equal to the value of D_{max}. The maximum value of the diameter in the equatorial plane, D_{eq}, can be estimated from Fig. 5c as the r value at which $P(r)$ is the maximum value: the mode of the $P(r)$ distribution (Table 1). The full width at half maximum also grows in the order from methyl to ethyl and *n*-propyl derivatives of poly(2-oxazolines) (Fig. 5c); that is, the IPC size distribution is broadened. Consequently, the supramolecular structure of the IPC becomes more dispersed.

A qualitative assessment of the IPC conformation is enabled by the analysis of Kratky plots ($q^2I(q)$ as the function of q) in normalized scattering intensity [79] (Fig. 5b). The presence of a well-defined peak signifies the polymer system's behavior akin to that of a particle, as previously discussed in [79,81,82], with the complexes under investigation having definable surfaces and attaining a globular particle-like structure. For globular particles, the peak maximum in normalized scattering intensity corresponds to the following coordinates: ($\sqrt{3}$; 1.1) as illustrated by the dotted lines in Fig. 5b. The subsequent increase in the normalized scattering intensity at larger qR_g is indicating the flexibility (the ability to undergo deformations) of the formed structure of the IPC. According to the authors [81], a high crosslinking density of more than 0.8 % is observed in such systems, which indicates the effective ability of PMAA and PAOx to form hydrogen bonds. Concurrently, these complexes exhibit hydrophilic properties at low values of n (Fig. 1), thereby manifesting a nanogel morphology.

The value of the Porod exponent, ν, was determined by approximating the SAXS curves by Eq. 4 for the complex formed between PMOx and PMAA. This yielded the supramolecular structure of the surface fractal with a fractal dimension, d_s, equal to 2.014 ± 0.003 (Table 1). However, it should be noted that the value of ν in this case is close to 4, and one can talk about a surface that clearly delimits the region of uniform distribution of the IPC particles from the solvent, with scattering following the Porod law ($I \sim q^{-4}$) nicely. Conversely, for the complexes of PEOx/PMAA and PnPOx/PMAA, a diffuse interfacial layer with a degree index β equal to 0.35 and 0.16, respectively, was obtained (Table 1). The expression of the density of the substance within this layer is as follows [84]:

$$\left\{ \begin{array}{c} \rho(x) = 0, x < 0 \\ \rho(x) = \rho_0 (x/a)^{\beta}, 0 \le x \le a \\ \rho(x) = \rho_0, a \le x \end{array} \right\} \quad (7)$$

Here x denotes the distance from a point within the inhomogeneity to the point on its boundary, while a represents the width of the diffuse interphase layer. Within this layer, the scattering density undergoes an increase from zero to ρ_0 in accordance with a power law, with an exponent of $0 \le \beta \le 1$. It is evident that when $\beta = 0$, a sharp phase boundary is evident at $x = 0$ in the experiment, manifesting as scattering according to the Porod law with a value of $\nu = 4$. This indicates an increase in the density of the polymer, $\rho(x)$, from the boundary $x = 0$. When β is increased to 1, the interfacial layer is eroded, leading to a linear increase in the substance's density from 0 to ρ_0 over a thickness x ranging from 0 to a.

The analysis of SAXS data has led to the conclusion that the IPCs formed in water exist as a highly cross-linked macromolecular aggregate, with a density of physical cross-linking greater than 0.8 % [81]. This is evidenced by the presence of numerous macromolecules that collectively form the nanogel network structure, as illustrated in Scheme 1. The nodes of the polymer network are likely to exist as the multiply-stranded structures of the PAOx and PMAA macromolecules, stabilized primarily by multiple hydrogen bonds (Scheme 1c and E3 in Supporting information) and additionally stabilized due to hydrophobic interactions of α-methyl groups in PMAA and alkyl groups in PAOx. This phenomenon leads to a corresponding increase in the radii of gyration for ellipsoid-like structures within the series of methyl-, ethyl-, and *n*-propyl moieties (Scheme S1).

Linear fragments of the polymer network contribute to a variable polymer density within the pores of the nanogels, as reflected in the Porod exponent, ν, exceeding 4 for complexes formed with PAOx containing ethyl and *n*-propyl groups (Table 1). It was found that the density of the substance $\rho(x)$ in the interfacial ("transition") layer increases for the PnPOx/PMAA ($\beta = 0.16$) faster than for PEOx/PMAA, where $\beta = 0.35$ (Eq. (7)). This is due to the larger lateral group size in PnPOx compared to PEOx. Instead of a diffuse layer between the polymer nanogel and the solvent for PMOx/PMAA, a hierarchical level with a supramolecular surface fractal structure with a dimension $d_s = 2.014$ ($\nu = 3.986$) is likely to exist between the IPC and the solvent, although the notion of a sharp boundary cannot be dismissed.

It is worthwhile to compare the behavior of the systems investigated in this study with the fractal characteristics of polymer systems possessing complex architectures. In the study by Lezov et al. [67], temperature-responsive star-shaped poly(2-ethyl-2-oxazoline) (star-PETOX) and poly(2-isopropyl-2-oxazoline) (star-PIPOX), with polymer arms grafted onto the lower rim of thiacalix[4]arene, were examined. At the supramolecular level of calixarene associates, the formation of mass fractals was observed, with fractal dimensions of 2.6 and 2.9 for star-PETOX and star-PIPOX, respectively. This contrasts with the nanogel networks reported in the present study, which exhibit a more diffuse structural organization. Moreover, at a higher level of supramolecular organization, the calixarene-based systems demonstrated a tendency to form compact, surface fractal structures with a fractal dimension of 2.9 [67].

4. Conclusions

A comparison between the structural data obtained by SAXS in a wide range of momentum transferred, and the nanosecond dynamics studied by polarized luminescence reveals a correlation between the

dynamics of component interactions and the structure of the IPC appearing in solution. SAXS analysis of aqueous solutions of PAOx/PMAA complexes has revealed the presence of at least one hierarchical level of supramolecular structure, which can be interpreted as a nanohydrogel structure. At the first hierarchical level, compact structures are formed with a characteristic size ranging from 40 to 10.7 nm. Within the hydrogen-bonding network of the IPC, poly(2-alkyl-2-oxazoline) (PAOx) has been identified as a key contributor to the compactness of the resulting supramolecular nanohydrogel structure. PAOx/PMAA complexes show promise for drug delivery applications due to their pH-responsive behavior, enabling controlled dissolution and drug release at targeted pH conditions, such as those found in specific regions of the gastrointestinal tract. Further research should focus on understanding the effects of pH on the formation of these complexes in aqueous environments and on the comprehensive characterization of their properties in solid state.

Declaration of Generative AI and AI-assisted technologies in the writing process

During the preparation of this work the author(s) used ChatGPT (OpenAI) to assist with the clarity and flow of some parts of the manuscript. After using this tool/service, the author(s) reviewed and edited the content as needed and take(s) full responsibility for the content of the publication.

CRediT authorship contribution statement

Ruslan Y. Smyslov: Writing – review & editing, Writing – original draft, Visualization, Validation, Resources, Methodology, Investigation, Formal analysis, Data curation. **Yulia E. Gorshkova:** Writing – original draft, Validation, Resources, Project administration, Methodology, Investigation, Funding acquisition, Formal analysis, Data curation. **Tatiana N. Nekrasova:** Methodology, Investigation. **Danelya N. Makhayeva:** Resources, Methodology, Investigation. **Grigoriy A. Mun:** Resources, Formal analysis. **Galiya S. Irmukhametova:** Supervision, Resources, Project administration, Funding acquisition. **Vitaliy V. Khutoryanskiy:** Writing – review & editing, Supervision, Resources, Conceptualization.

Funding

The SAXS experiments were conducted as part of the scientific project 04–4-1149–2-2021/2028, with financial support from the JINR—Republic of Kazakhstan cooperation program in 2024-2025 (Project 448 dated 06.06.2024, clause 6 and Project 36 dated 23.01.2025, clause 4). DNM, GSI, GAM and VVK acknowledge the Committee of Science of the Ministry of Science and Higher Education of the Republic of Kazakhstan (Grant No BR24993113). Additionally, VVK acknowledges the Royal Society for his industry fellowship (IF\R2 \222031).

Declaration of competing interest

The authors declare the following financial interests/personal relationships which may be considered as potential competing interests: Yulia E. Gorshkova and Galiya S. Irmukhametova report financial support was provided by Joint Institute for Nuclear Research — Republic of Kazakhstan cooperation program. Danelya N. Makhayeva, Grigoriy A. Mun, Galiya S. Irmukhametova, and Vitaliy V. Khutoryanskiy report financial support was provided by Committee of Science of the Ministry of Science and Higher education of the Republic of Kazakhstan. Vitaliy V. Khutoryanskiy reports financial support was provided by The Royal Society. If there are other authors, they declare that they have no known competing financial interests or personal relationships that could have appeared to influence the work reported in this paper.

Acknowledgements

The software used in this study is SasView, which was originally developed as part of the National Science Foundation (NSF) DMR-0520547 Award. Additionally, SasView incorporates code developed with financial support from the European Union's Horizon 2020 research and innovation program under the SINE2020 Grant No. 654000 project. The authors acknowledge Dr Marina A. Bezrukova for determination of the molecular weight of PMAA by sedimentation and diffusion methods.

Appendix A. Supplementary data

Supplementary data to this article can be found online at https://doi.org/10.1016/j.jcis.2025.138185.

Data availability

Data will be made available on request.

References

[1] V.V. Khutoryanskiy, R.Y. Smyslov, A.V. Yakimansky, Modern Methods for Studying Polymer Complexes in Aqueous and Organic Solutions, *Polym. Sci., Ser. A* 60 (2018) 553–576, https://doi.org/10.1134/S0965545X18050085.
[2] I.M. Papisov, A.A. Litmanovich, Molecular "recognition" in interpolymer interactions and matrix polymerization, in: Conducting Polymers/Molecular Recognition. Advances in Polymer Science 90, Springer, Berlin, Heidelberg, 1989, https://doi.org/10.1007/3-540-51096-6_3.
[3] E. Tsuchida, K. Abe, in: E. Tsuchida, K. Abe (Eds.), Interactions Between Macromolecules in Solution and Intermacromolecular Complexes. Advances in Polymer Science, 45, Springer, Berlin, Heidelberg, 1982, https://doi.org/10.1007/BFb0017549.
[4] E.A. Bekturov, L.A. Bimendina, Interpolymer complexes, in: Speciality Polymers. Advances in Polymer Science, vol 41, Springer, Berlin, Heidelberg, 1981, https://doi.org/10.1007/3-540-10554-9_11.
[5] S. Lankalapalli, V.R.M. Kolapalli, Polyelectrolyte complexes: a review of their applicability in drug delivery technology, Indian J. Pharm. Sci. 71 (5) (2009) 481–487, https://doi.org/10.4103/0250-474X.58165. PMID: 20502564; PMCID: PMC2866337.
[6] M.H.A. Azqhandi, B.V. Farahani, N. Dehghani, Encapsulation of methotrexate and cyclophosphamide in interpolymer complexes formed between poly acrylic acid and poly ethylene glycol on multi-walled carbon nanotubes as drug delivery systems, Mater. Sci. Eng. C 79 (2017) 841–847, https://doi.org/10.1016/j.msec.2017.05.089.
[7] C.L. Bell, N.A. Peppas, Biomedical membranes from hydrogels and interpolymer complexes, in: N.A. Peppas, R.S. Langer (Eds.), Biopolymers II. Advances in Polymer Science, vol 122, Springer, Berlin, Heidelberg, 1995, https://doi.org/10.1007/3540587888_15.
[8] V.A. Izumrudov, B.K. Mussabayeva, Z.S. Kassymova, A.N. Klivenko, L. K. Orazzhanova, Interpolyelectrolyte complexes: advances and prospects of application, Russ. Chem. Rev. 88 (10) (2019) 1046, https://doi.org/10.1070/RCR4877.
[9] Basic Properties of Soluble Interpolyelectrolyte Complexes Applied to Bioengineering and Cell Transformations P. 151 (1994), https://doi.org/10.1007/978-3-642-78469-9_10.
[10] E.V. Kukhtenko, F.V. Lavrentev, V.V. Shilovskikh, P.I. Zyrianova, S.I. Koltsov, A. S. Ivanov, A.S. Novikov, A.A. Muravev, K.G. Nikolaev, D.V. Andreeva, et al., Periodic Self-Assembly of Poly(ethyleneimine)–poly(4-styrenesulfonate) complex Coacervate Membranes, Polymers 15 (2023) 45, https://doi.org/10.3390/polym15010045.
[11] K.G. Nikolaev, S.A. Ulasevich, O. Luneva, O.Y. Orlova, D. Vasileva, S. Vasilev, A. S. Novikov, E.V. Skorb, Humidity-driven transparent holographic free-standing polyelectrolyte films, ACS Appl. Polym. Mater. 2 (2) (2020) 105–112, https://doi.org/10.1021/acsapm.9b01151.
[12] H. Dautzenberg, N. Karibyants, Polyelectrolyte complex formation in highly aggregating systems. Effect of salt: response to subsequent addition of NaCl, Macromol. Chem. Phys. 200 (1) (1999) 118–125, https://doi.org/10.1002/(SICI)1521-3935(19990101)200:1%3C118::AID-MACP118%3E3.0.CO;2-K.
[13] O.S. Brovko, I.A. Palamarchuk, T.A. Boitsova, et al., Influence of the conformation of biopolyelectrolytes on the morphological structure of their interpolymer complexes, Macromol. Res. 23 (2015) 1059–1067, https://doi.org/10.1007/s13233-015-3140-z.
[14] M.G. Krakovyak, T.D. Ananieva, E.V. Anufrieva, Bridge Bond Formation in Polymer Systems, Journal of Macromolecular Science, Part C 33 (2) (1993) 181–236, https://doi.org/10.1080/15321799308021562.
[15] V.V. Khutoryanskiy, Hydrogen-bonded interpolymer complexes as materials for pharmaceutical applications, Int. J. Pharm. 334 (1–2) (2007) 15–26, https://doi.org/10.1016/j.ijpharm.2007.01.037.

[16] S. Luo, S. Liu, J. Xu, H. Liu, Z. Zhu, M. Jiang, C. Wu, A stopped-flow kinetic study of the assembly of interpolymer complexes via hydrogen-bonding interactions, Macromolecules 39 (13) (2006) 4517–4525, https://doi.org/10.1021/ma060581y.
[17] H. Tsuji, Poly(lactic acid) stereocomplexes: a decade of progress, Adv. Drug Deliv. Rev. (2016), https://doi.org/10.1016/j.addr.2016.04.017.
[18] E.V. Anufrieva, M.G. Krakovyak, T.N. Nekrasova, R.Y. Smyslov, Stereocomplexes of poly(methacrylic acid) and poly(methyl methacrylate), Polym. Sci., Ser. B 43 (7) (2001) 230–231.
[19] E.V. Anufrieva, M.G. Krakovyak, T.N. Nekrasova, R.Y. Smyslov, Effect of solvent on the formation of stereocomplexes in poly (methyl methacrylate) solutions, Polym. Sci., Ser. A 38 (2) (1996) 190–193.
[20] E.V. Anufrieva, M.G. Krakovyak, T.N. Nekrasova, V.B. Lushchik, R.Y. Smyslov, Influence of the degree of stereoregularity of isotactic and syndiotactic polymethyl methacrylates on formation of stereopoly complexes in various solvents, Russ. J. Appl. Chem. 69 (6) (1996) 886–889.
[21] M.F. Budyka, A.G. Rachinsky, M.V. Alfimov, Donor—acceptor complexes: the model of unlimited co-aggregation or polycomplexes formation, Chem. Phys. Lett. 181 (1) (1991) 59–62, https://doi.org/10.1016/0009-2614(91)90221-T.
[22] G.B. Sukhorukov, E. Donath, H. Lichtenfeld, E. Knippel, M. Knippel, A. Budde, H. Möhwald, Layer-by-layer self assembly of polyelectrolytes on colloidal particles, Colloids Surf A Physicochem Eng Asp 137 (1–3) (1998) 253–266.
[23] J.J. Richardson, J. Cui, M. Bjornmalm, J.A. Braunger, H. Ejima, F. Caruso, Innovation in layer-by-layer assembly, Chem. Rev. 116 (23) (2016) 14828–14867, https://doi.org/10.1021/acs.chemrev.6b00627.
[24] S.E. Kudaibergenov, R.E. Khamzamulina, E.A. Bekturov, L.A. Bimendina, V. A. Frolova, M.Z. Askarova, Polyelectrolyte complex formation on a dimeric interface, Macromol. Rapid Commun. 15 (12) (1994) 943–947, https://doi.org/10.1002/marc.1994.030151206.
[25] A. Murmiliuk, H. Iwase, J.J. Kang, S. Mohanakumar, M.S. Appavou, K. Wood, A. Radulescu, Polyelectrolyte-protein synergism: pH-responsive polyelectrolyte/insulin complexes as versatile carriers for targeted protein and drug delivery, J. Colloid Interface Sci. 665 (2024) 801–813.
[26] K.L. Smith, A.E. Winslow, D.E. Petersen, Association reactions for poly(alkylene oxides) and polymeric poly(carboxylic acids), Ind. Eng. Chem. 51 (11) (1959) 1361–1364.
[27] S. Zou, R. Lv, Z. Tong, B. Na, K. Fu, H. Liu, In situ hydrogen-bonding complex mediated shape memory behavior of PAA/PEO blends, Polymer 183 (2019) 121878, https://doi.org/10.1016/j.polymer.2019.121878.
[28] T. Miyoshi, K. Takegoshi, K. Hikichi, High-resolution solid state 13C nmr study of the interpolymer interaction, morphology and chain dynamics of the poly (acrylic acid)/poly (ethylene oxide) complex, Polymer 38 (10) (1997) 2315–2320.
[29] R.F. Schmidt, J. Lutzki, R. Dalgliesh, S. Prévost, M. Gradzielski, pH-Responsive Rheology and Structure of Poly (ethylene oxide)–Poly (methacrylic acid) Interpolymer Complexes, Macromolecules 58 (1) (2025) 321–333, https://doi.org/10.1021/acs.macromol.4c02726.
[30] Z.S. Nurkeeva, G.A. Mun, A.V. Dubolazov, V.V. Khutoryanskiy, pH Effects on the Complexation, Miscibility and Radiation-Induced Crosslinking in Poly (acrylic acid)-Poly (vinyl alcohol) Blends, Macromol. Biosci. 5 (5) (2005) 424–432, https://doi.org/10.1002/mabi.200400200.
[31] G. Staikos, K. Karayanni, Y. Mylonas, Complexation of polyacrylamide and poly (N-isopropylacrylamide) with poly (acrylic acid). the temperature effect, Macromol. Chem. Phys. 198 (9) (1997) 2905–2915, https://doi.org/10.1002/macp.1997.021980920.
[32] G.A. Mun, Z.S. Nurkeeva, V.V. Khutoryanskiy, G.S. Sarybayeva, A.V. Dubolazov, pH-effects in the complex formation of polymers I. Interaction of poly (acrylic acid) with poly (acrylamide), Eur. Polym. J. 39 (8) (2003) 1687–1691.
[33] L. Ruiz-Rubio, J.M. Laza, L. Pérez, et al., Polymer–polymer complexes of poly(N-isopropylacrylamide) and poly(N,N-diethylacrylamide) with poly(carboxylic acids): a comparative study, Colloid Polym. Sci. 292 (2014) 423–430, https://doi.org/10.1007/s00396-013-3086-7.
[34] Z.S. Nurkeeva, G.A. Mun, V.V. Khutoryanskiy, A.B. Bitekenova, A.V. Dubolazov, S. Z. Esirkegenova, pH effects in the formation of interpolymer complexes between poly (N-vinylpyrrolidone) and poly (acrylic acid) in aqueous solutions, The European Physical Journal E 10 (2003) 65–68, https://doi.org/10.1140/epje/e2003-00003-4.
[35] R. Subramanian, P. Natarajan, Interaction between poly (N-vinylpyrrolidone) and poly (acrylic acid) s: influence of hydrogen and cupric ions on the adduct formation, J. Polym. Sci., Polym. Chem. Ed. 22 (2) (1984) 437–451, https://doi.org/10.1002/pol.1984.170220215.
[36] A. Henke, S. Kadłubowski, M. Wolszczak, P. Ulański, V. Boyko, T. Schmidt, J. M. Rosiak, The Structure and Aggregation of Hydrogen-Bonded Interpolymer Complexes of Poly (acrylic acid) with Poly (N-vinylpyrrolidone) in Dilute Aqueous solution, Macromol. Chem. Phys. 212 (23) (2011) 2529–2540, https://doi.org/10.1002/macp.201100409.
[37] D.M. Kandhasamy, C. Selvaraju, V. Dharuman, Structure and dynamics of poly (methacrylic acid) and its interpolymer complex probed by covalently bound rhodamine-123, Spectrochim. Acta A Mol. Biomol. Spectrosc. 248 (2021) 119166.
[38] O.V. Khutoryanskaya, A.C. Williams, V.V. Khutoryanskiy, pH-mediated interactions between poly (acrylic acid) and methylcellulose in the formation of ultrathin multilayered hydrogels and spherical nanoparticles, Macromolecules 40 (21) (2007) 7707–7713, https://doi.org/10.1021/ma071644v.
[39] K. Karayanni, G. Staikos, Study of the lower critical solution temperature behaviour of poly (vinyl methyl ether) aqueous solutions in the presence of poly (acrylic acid). the role of interpolymer hydrogen bonding interaction, Eur. Polym. J. 36 (12) (2000) 2645–2650.
[40] S.C. Bizley, A.C. Williams, V.V. Khutoryanskiy, Thermodynamic and kinetic properties of interpolymer complexes assessed by isothermal titration calorimetry and surface plasmon resonance, Soft Matter 10 (2014) 8254, https://doi.org/10.1039/c4sm01138d.
[41] E.V. Anufrieva, M.G. Krakovyak, T.N. Nekrasova, R.Y. Smyslov, Polarized luminescence and nanosecond dynamics in the studies of interpolymer complexes, in: Vitaliy V. Khutoryanskiy, Georgios Staikos (Eds.), Hydrogen Bonded Interpolymer Complexes: Formation, Structure and Applications, 2009, pp. 69–83. ISBN 978-981-270-977-6. OCLC 613658891. https://doi.org/10.1142/6498.
[42] T. Nekrasova, O. Nazarova, E. Vlasova, A. Fischer, Y. Zolotova, M. Bezrukova, E. Panarin, Interpolymer Complexes of Poly(methacryloyloxyethyl phosphorylcholine) and Polyacids, Polymers 14 (2022) 407, https://doi.org/10.3390/polym14030407.
[43] T. Benselfelt, G. Cinar Ciftci, L. Wågberg, J. Wohlert, M.M. Hamedi, Entropy drives interpolymer association in water: insights into molecular mechanisms, Langmuir 40 (13) (2024) 6718–6729, https://doi.org/10.1021/acs.langmuir.3c02978.
[44] R. Hoogenboom, Poly(2-oxazoline)s: a polymer class with numerous potential applications, Angew. Chem. Int. Ed. 48 (43) (2009) 7978–7994, https://doi.org/10.1002/anie.200901607.
[45] Mathias Glassner, Maarten Vergaelen, Poly(2-oxazoline)s: A comprehensive overview of polymer structures and their physical properties, Polymer Int. 67 (1) (2018) 32–45, https://doi.org/10.1002/pi.5457.
[46] R. Hoogenboom, The future of poly (2-oxazoline)s, Eur. Polym. J. 179 (2022) 111521, https://doi.org/10.1016/j.eurpolymj.2022.111521.
[47] N. Adams, U.S. Schubert, Adv. Drug Deliv. Rev. 59 (2007) 1504–1520, https://doi.org/10.1016/j.addr.2007.08.018.
[48] X. Shan, S. Aspinall, D.B. Kaldybekov, F. Buang, A.C. Williams, V.V. Khutoryansky, Synthesis and evaluation of methacrylated poly (2-ethyl-2-oxazoline) as a mucoadhesive polymer for nasal drug delivery, ACS Appl. Polym. Mater. 3 (11) (2021) 5882–5892, https://doi.org/10.1021/acsapm.1c010.
[49] O. Sedlacek, B.D. Monnery, S.K. Filippov, R. Hoogenboom, M. Hruby, Poly (2-Oxazoline) s–Are they more Advantageous for Biomedical applications than Other Polymers? Macromol. Rapid Commun. 33 (19) (2012) 1648–1662, https://doi.org/10.1002/marc.201200453.
[50] J.M. Harris, M.D. Bentley, R.W. Moreadith, T.X. Viegas, Z. Fang, K. Yoon, L. Nordstierna, Tuning drug release from polyoxazoline-drug conjugates, Eur. Polym. J. 120 (2019) 109241, https://doi.org/10.1016/j.eurpolymj.2019.109241.
[51] A.R. Salgarella, A. Zahoranová, P. Šrámková, et al., Investigation of drug release modulation from poly(2-oxazoline) micelles through ultrasound, Sci. Rep. 8 (2018) 9893, https://doi.org/10.1038/s41598-018-28140-3.
[52] L. Simon, M. Vincent, S. Le Saux, V. Lapinte, N. Marcotte, M. Morille, S. Bégu, Polyoxazolines based mixed micelles as PEG free formulations for an effective quercetin antioxidant topical delivery, *Int. J. Pharm.* 570 (2019) 118516, https://doi.org/10.1016/j.ijpharm.2019.118516.
[53] M. Hruby, S.K. Filippov, J. Panek, M. Novakova, H. Mackova, J. Kucka, K. Ulbrich, Polyoxazoline thermoresponsive micelles as radionuclide delivery systems, Macromol. Biosci. 10 (8) (2010) 916–924.
[54] R. Hoogenboom, H. Schlaad, Thermoresponsive poly(2-oxazoline)s, polypeptoids, and polypeptides, *Polym. Chem.* 8 (1) (2017) 24–40.
[55] H. Fael, C. Ràfols, A.L. Demirel, Poly (2-ethyl-2-oxazoline) as an alternative to poly (vinylpyrrolidone) in solid dispersions for solubility and dissolution rate enhancement of drugs, J. Pharm. Sci. 107 (9) (2018) 2428–2438, https://doi.org/10.1016/j.xphs.2018.05.015.
[56] X. Shan, A.C. Williams, V.V. Khutoryanskiy, Polymer structure and property effects on solid dispersions with haloperidol: Poly (N-vinyl pyrrolidone) and poly (2-oxazolines) studies, Int. J. Pharm. 590 (2020) 119884, https://doi.org/10.1016/j.ijpharm.2020.119884.
[57] G.K. Abilova, S.F. Nasibullin, K. Ilyassov, A.N. Adilov, M.K. Akhmetova, R. I. Moustafine, V.V. Khutoryanskiy, Mucoadhesive gellan gum/poly (2-ethyl-2-oxazoline) films for ocular delivery of pilocarpine hydrochloride, J. Drug Delivery Sci. Technol. 104 (2025) 106492, https://doi.org/10.1016/j.jddst.2024.106492.
[58] L. Trachsel, M. Zenobi-Wong, E.M. Benetti, The role of poly(2-alkyl-2-oxazoline)s in hydrogels and biofabrication (Minireview) Biomater, Sci., 9 (2021) 2874–2886, https://doi.org/10.1039/D0BM02217A.
[59] A.M. Kelly, F. Wiesbrock, Strategies for the Synthesis of Poly(2-Oxazoline)-based Hydrogels, Macromol. Rapid Commun. 33 (2012), https://doi.org/10.1002/marc.201200333.
[60] D.N. Makhayeva, S.K. Filippov, S.S. Yestemes, G.S. Irmukhametova, V. V. Khutoryanskiy, Polymeric iodophors with poly (2-ethyl-2-oxazoline) and poly (N-vinylpyrrolidone): Optical, hydrodynamic, thermodynamic, and antimicrobial properties, Eur. Polym. J. 165 (2022) 111005, https://doi.org/10.1016/j.eurpolymj.2022.111005.
[61] R.I. Moustafine, A.S. Viktorova, V.V. Khutoryanskiy, Interpolymer complexes of carbopol® 971 and poly (2-ethyl-2-oxazoline): Physicochemical studies of complexation and formulations for oral drug delivery, *Int. J. Pharm.* 558 (2019) 53–62, https://doi.org/10.1016/j.ijpharm.2019.01.002.
[62] L. Ruiz-Rubio, M.L. Alonso, L. Pérez-Álvarez, R.M. Alonso, J.L. Vilas, V. V. Khutoryanskiy, Formulation of Carbopol®/Poly (2-ethyl-2-oxazoline) s mucoadhesive tablets for buccal delivery of hydrocortisone, *Polymers* 10 (2) (2018) 175, https://doi.org/10.3390/polym10020175.
[63] E.B. Adatoz, S. Hendessi, C.W. Ow-Yang, A.L. Demirel, Restructuring of poly (2-ethyl-2-oxazoline)/tannic acid multilayers into fibers, *Soft Matter* 14 (19) (2018) 3849–3857.
[64] C. Su, J. Sun, X. Zhang, D. Shen, S. Yang, Hydrogen-bonded polymer complex thin film of poly (2-oxazoline) and poly (acrylic acid), *Polymers* 9 (8) (2017) 363, https://doi.org/10.3390/polym9080363.

[65] Q.D. Dang, J.R. Moon, Y.S. Jeon, J.H. Kim, Supramolecular adhesive gels based on biocompatible poly (2-ethyl-2-oxazoline) and tannic acid via hydrogen bonding complexation, *J. Appl. Polym. Sci.* 137 (3) (2020) 48285, https://doi.org/10.1002/app.48285.

[66] V.D. Pautov, T.N. Nekrasova, T.D. Anan'eva, R.Y. Smyslov, Polarized Luminescence Studies of Nanosecond Dynamics of Thermosensitive Polymers in Aqueous Solutions, in: Vitaliy V. Khutoryanskiy, Theoni K. Georgiou (Eds.), Temperature-responsive Polymers: Chemistry, Properties, and Applications, first ed., JohnWiley & Sons Ltd., 2018, ISBN 978-1-119-15778-6, pp. 249–278, https://doi.org/10.1002/9781119157830.ch10 (Chapter 10).

[67] A.A. Lezov, A.S. Gubarev, A.N. Podsevalnikova, et al., Temperature-responsive star-shaped poly(2-ethyl-2-oxazoline) and poly(2-isopropyl-2-oxazoline) with central thiacalix[4]arene fragments: structure and properties in solutions, *Colloid Polym. Sci.* 297 (2019) 285–296, https://doi.org/10.1007/s00396-018-4458-9.

[68] A.A. Lezov, A.S. Gubarev, M.E. Mikhailova, A.A. Lezova, N.G. Mikusheva, V. D. Kalganov, M.M. Dudkina, A.A. Ten'kovtsev, T. Nekrasova, L.N. Andreeva, N. N. Saprykina, R.Y. Smyslov, Y.E. Gorshkova, D.P. Romanov, S. Höppener, I. Perevyazko, N.V. Tsvetkov, Star-Shaped Poly(2-ethyl-2-oxazoline) and Poly(2-isopropyl-2-oxazoline) with Central Thiacalix[4]Arene Fragments: Reduction and Stabilization of Silver Nanoparticles, Polymers 11 (12) (2019) 2006, https://doi.org/10.3390/polym11122006.

[69] O. Sedlacek, B.D. Monnery, R. Hoogenboom, Synthesis of defined high molar mass poly (2-methyl-2-oxazoline), Polym. Chem. 10 (11) (2019) 1286–1290, https://doi.org/10.1039/C9PY00013E.

[70] *Tsvetkov, V.N.* Rigid-Chain Polymers: Hydrodynamic and Optical Properties in Solution; Macromolecular Compounds; Consultants Bureau: New York, NY, USA, 1989; ISBN 978-0-306-11020-7.

[71] Régis David. Biophysique. 1/Biophysique générale. Presses universitaires de France. 1re éd. 1992; ISBN-13 978-2130361718.

[72] E.V. Anufrieva, Y.Y. Gotlib, Investigation of polymers in solution by polarized luminescence, in: Luminescence. Advances in Polymer Science, vol 40, Springer, Berlin, Heidelberg, 1981, https://doi.org/10.1007/3-540-10550-6_1.

[73] L. Swanson, Optical Properties of Polyelectrolytes, in: Norman S. Allen (Ed.), Photochemistry and Photophysics of Polymer Materials, 2010, pp. 41–91, https://doi.org/10.1002/9780470594179.ch2.

[74] G.A. Mun, Z.S. Nurkeeva, V.V. Khutoryanskiy, A.B. Bitekenova, Effect of copolymer composition on interpolymer complex formation of (co) poly (vinyl ether) s with poly (acrylic acid) in aqueous and organic solutions, Macromol. Rapid Commun. 21 (7) (2000) 381–384, https://doi.org/10.1002/(SICI)1521-3927(20000401)21:7<381::AID-MARC381>3.0.CO;2-B.

[75] G. Beaucage, Approximations leading to a unified exponential/power-law approach to small-angle scattering, *Applied Crystallography* 28 (6) (1995) 717–728, https://doi.org/10.1107/S0021889895005292.

[76] *M. Doucet, et al.* SasView Version 4.2.2 http://doi.org/10.5281/zenodo.2652478.

[77] D.I. Svergun, M.H.J. Koch, Small-angle scattering studies of biological macromolecules in solution, Reports Prog. Phys. 66 (2003) 1735–1782, https://doi.org/10.1088/0034-4885/66/10/R05.

[78] L.A. Feigin, D.I. Svergun, G.W. Taylor, Determination of the Integral Parameters of Particles, in: G.W. Taylor (Ed.), Structure Analysis by Small-Angle X-Ray and Neutron Scattering, Springer, Boston, MA, 1987, https://doi.org/10.1007/978-1-4757-6624-0_3.

[79] A.G. Kikhney, D.I. Svergun, *A practical guide to small angle X-ray scattering (SAXS) of flexible and intrinsically disordered proteins*, *FEBS Lett.* 589 (19PartA) (2015) 2570–2577, https://doi.org/10.1016/j.febslet.2015.08.027.

[80] J. Pérez, P. Vachette, D. Russo, M. Desmadril, D. Durand, Heat-induced unfolding of neocarzinostatin, a small all-β protein investigated by small-angle X-ray scattering 1 1Edited by M F. Moody, J. Mol. Biol. 308 (4) (2001) 721–743, https://doi.org/10.1006/jmbi.2001.4611.

[81] Lu. Jacob Fischer, T.S. Han, M. Dadmun, When does a macromolecule transition from a polymer chain to a nanoparticle? Nanoscale Adv. 4 (2022) 5164–5177, https://doi.org/10.1039/D2NA00617K.

[82] V.M. Burger, et al., A Structure-free Method for Quantifying Conformational Flexibility in proteins, Sci. Rep. 6 (2016) 29040, https://doi.org/10.1038/srep29040.

[83] P.W. Schmidt, Small-angle scattering studies of disordered, porous and fractal systems, Applied Crystallography 24 (5) (1991) 414–435.

[84] P.W. Schmidt, D. Avnir, D. Levy, A. Höhr, M. Steiner, A. Röll, Small-angle X-ray scattering from the surfaces of reversed-phase silicas: Power-law scattering exponents of magnitudes greater than four, J. Chem. Phys. 94 (2) (1991) 1474–1479, https://doi.org/10.1063/1.460006.